I.A.H. AJEEL,[1] M.J.R. ALDHUHAIBAT,[1] K.S. JASSIM[2]

[1] Department of Physics, College of Science, University of Wasit
(Wasit, Iraq)

[2] Department of Physics, College of Education for pure Sciences, University of Babylon
(PO Box 4, Hilla-Babylon, Iraq; e-mail: khalidsj@uobabylon.edu.iq)

COULOMB C2 AND C4 FORM FACTORS OF ^{18}O, ^{20,22}Ne NUCLEI USING BOHR–MOTTELSON COLLECTIVE MODEL

UDC 539

Coulomb C2 and C4 form factors with core-polarization effects to 2^+ and 4^+ states in ^{18}O and $^{20,22}Ne$ have been studied using shell model calculations. The two-body effective Wildenthal interaction and universal sd-shell interaction A (USDA) are used for sd-shell orbits. Core-polarization effects are calculated using the Coulomb valance Tassie model (CVTM) and Bohr–Mottelson (BM) collective model. Some wave functions of the radial single-particle matrix elements have been calculated with harmonic oscillator (HO), Wood–Saxon (WS), and SKX potentials. The inclusions of core-polarization effects give good agreements with experimental data as comparing with model space calculations. The results for different potentials are compared.

K e y w o r d s: *sd*-shell nuclei, longitudinal form factors, Coulomb form factors, Nushellx@MUS code.

1. Introduction

The shell model remains the important theoretical tool for understanding the properties of nuclei. It can be used to provide the qualitative understanding in its simplest single-particle form, but it is also used as a basis for calculations that are much more complex and complete. The expansion of its application seems to be limited in the near future. The shell model takes a particularly important position, basically because the shell model is a more fundamental framework based on a minimum number of assumptions in addition to the fact that the shell model has been extremely successful in describing the light nuclei at low excitation energies. The shell-model assumption says that we can separate the system into a core part and a valence part, and describe the interaction between the core and the valence particle, and that among the valence particles. The interaction between them will excite the core. This process, known as the core excitation, will then give rise to an effective force between the valence particles, since two of them will have their state to be shifted as a consequence of their interaction with the core, while the core has returned to the original state. This process can be described as a polarization of the core by one of the valence particles. The scattering of high-energy electrons by the nucleus is very useful as a means of elucidating the nuclear structure [1]. Nuclear size estimates were made using the scattering energy below 50 MeV, but the most significant contributions were made to electron energies in the interval 100 to 900 MeV, so that the amount of information that can be extracted from the energy electron scattering depends on the magnitude of the de Broglie wavelength of the incident electrons compared to the radius of the scattering nucleus, so that the electron acts as a probe for the study of the nuclear structure [1]. There are many reasons, why the electron-nucleus scattering is considered to be an excellent tool to study the nuclear structure. The basic interaction between the electron and the target nucleus is known. Since the interaction is relatively weak, one can make measurements on the target nucleus without greatly disturbing its structure. The universal sd-shell interaction (USD) Hamiltonian [2] provided realistic sd-shell ($1d_{5/2}$, $1d_{3/2}$) wave functions for use in nuclear structure models, nuclear spectroscopy, and nuclear astrophysics for over two decades. It is also an important part of the Hamiltonian used for the *p-sd* [3] and *sd-pf*

[4–6] model spaces[7]. The USD Hamiltonian is construct by 63 two-body matrix elements (TBME) and three single-particle energies (SPE) given in Table I of Ref. [8]. The USDA (universal sd-shell interaction A) interaction [7] is a new USD-type Hamiltonian based on 66 parameters to fit 608 energy data in sd-shell nuclei (A = 16–40) with a root mean square (rms) deviation of 130 KeV and 170 KeV, respectively [7]. This interaction has been resolved the fluorine problem and as well as all of the oxygen isotopes are unbound. The single-particle energies for USDB are 2.1117 MeV, –3.9257 MeV, and –3.2079 MeV for the $1d_{5/2}$, $1d_{3/2}$, and $2s_{1/2}$ orbitals. Richter and Brown [9] have made a comparison between the experimental and theoretical results of corresponding levels in ^{26}Mg levels based on energies, electron scattering form factor. Results based on the new *sd*-shell interactions USDA and USDB.

Coulomb form factors of C4 transitions in even-even $N = Z$ *sd*-shell nuclei (^{24}Mg, ^{28}Si and ^{32}S) have been investigated by R.A. Radhi [10] by involving the higher-energy configurations outside the sd-shell model space which are called core polarization effects. The calculated of Coulomb and longitudinal form factors with different model spaces have attracted much attention of many authors like in [11]. Some theoretical papers on electron scattering form factors in *p*-shell [12, 13], *sd* and *fp*-shells [14–17] and Sn isotopes [18] have been studied and give agreement comparing with experimental data.

2. Theory

The Tassie model (TM) used for the core polarization in Nushellx@MUS is a modeling of more elasticity and modification that allows a non-uniform mass and charge density distributions [13]. The polarization of the core (CP) charge density in TM model depends on the ground state charge density of the nucleus. The ground-state charge density is expressed in terms of the two-body charge density for all occupied shells including the core. Based on the collective modes of the nuclei, the Tassie shape CP transition density is given by [19],

$$\rho^{\rm core}_{Jt_z}(i,f,r) = \frac{1}{2}C(1+\tau_z)r^{J-1}\frac{d\rho_0(i,f,r)}{dr}, \qquad (1)$$

where C is a proportionality constant, and ρ_0 is the ground state two-body charge density distribution, which is given [21],

$$\rho_0 = \left\langle \psi|\hat{\rho}^{(2)}_{\rm eff}(\mathbf{r})|\psi\right\rangle = $$
$$= \sum_{i<j}\left\langle ij|\hat{\rho}^{(2)}_{\rm eff}(\mathbf{r})|ij\right\rangle - \left\langle ij|\hat{\rho}^{(2)}_{\rm eff}(\mathbf{r})|ij\right\rangle, \qquad (2)$$

where

$$\hat{\rho}^{(2)}_{\rm eff}(\mathbf{r}) = $$
$$= \frac{1}{2(A-1)}f(r_{ij})\sum_{i\neq j}\{\delta(\mathbf{r}-\mathbf{r}_i)+\delta(\mathbf{r}-\mathbf{r}_J)\}f(r_ij), \quad (3)$$

where i and j are all the required quantum numbers, i.e., the functions $f(r_{ij})$ are the two-body short-range correlation (SRC). In this work, a simple model form of short-range correlation has been adopted, i.e. [19],

$$f(r_{ij}) = 1 - \exp[-\beta(r_{ij}-r_c)^2], \qquad (4)$$

where r_c is the radius of a suitable hard core, and β is a correlation parameter.

The Coulomb form factor for this model becomes [20]:

$$F^L_J(q) = \sqrt{\frac{4\pi}{2J_i+1}}\frac{1}{Z}\left\{\int_0^\infty r^2 j_J(qr)\rho^{ms}_{Jt_z}(i,f,r)dr + \right.$$
$$\left. + C\int_0^\infty j_J(qr)r^{J+1}\frac{d\rho_0(i,f,r)}{dr}\,dr\right\}F_{cm}(q)F_{fc}(q) \qquad (5)$$

but,

$$\int_0^\infty j_J(qr)r^{J+1}\frac{d\rho_0(i,f,r)}{dr}\,dr =$$
$$= \int_0^\infty \frac{d}{dr}[j_J(qr)r^{J+1}\rho_0(i,f,r)]dr -$$
$$- \int_0^\infty (J+1)j_J(qr)r^J\rho_0(i,f,r)dr -$$
$$- \int_0^\infty \frac{dj_J(qr)}{dr}r^{J+1}\rho_0(i,f,r)dr, \qquad (6)$$

where the first term gives zero contribution, the second and third terms can be combined together as [19],

$$-q\int_0^\infty r^{J+1}\rho_0(i,f,r)\left[\frac{d}{d(qr)}+\frac{J+1}{qr}\right]j_J(qr)dr \qquad (7)$$

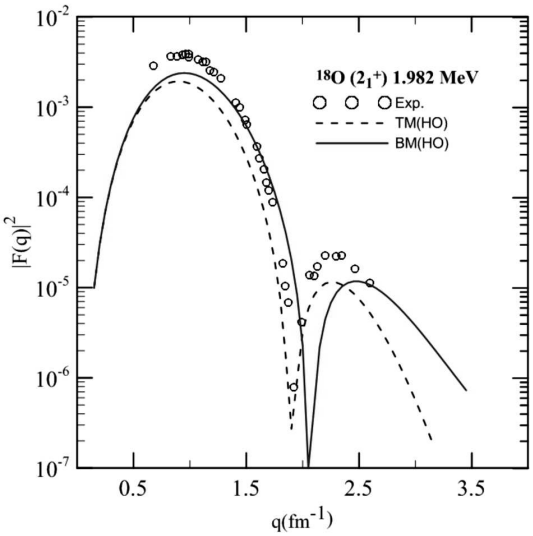

Fig. 1. The longitudinal C2 form factors for the transition of the 2_1^+ (1.982 MeV) state in ^{18}O, using the BM collective model and Tassie model with HO potential

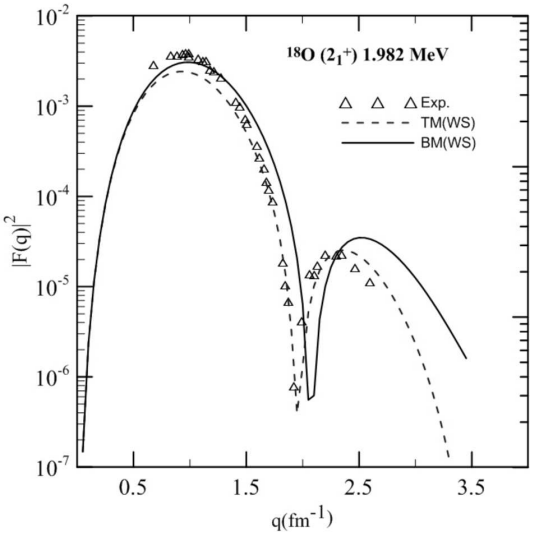

Fig. 2. The longitudinal C2 form factors for the transition of the 2_1^+ (1.982 MeV) state in ^{18}O, with the BM collective model and Tassie model, with Wood-Saxon (WS) potential

from the recursion of the spherical Bessel function [19],

$$\left[\frac{d}{d(qr)}+\frac{J+1}{qr}\right] j_J(qr) = j_{J-1}(qr), \tag{8}$$

$$\therefore \int_0^\infty j_J(qr) r^{J+1} \frac{d\rho_0(i,f,r)}{dr}\, dr =$$

$$= -q \int_0^\infty r^{J+1} \rho_0(i,f,r) j_{J-1}(qr)\, dr. \tag{9}$$

Therefore, the form factor of Eq. (5) takes the form [21]:

$$F_J^L(q) = \sqrt{\frac{4\pi}{2J_i+1}} \frac{1}{Z} \left\{ \int_0^\infty r^2 j_J(qr) \rho_{Jt_z}^{ms}(i,f,r) dr - \right.$$

$$\left. - qC \int_0^\infty r^{J+1} \rho_0(i,f,r) j_{J-1}(qr)\, dr \right\} F_{cm}(q) F_{fc}(q). \tag{10}$$

The proportionality constant C can be determined from the form factor evaluated at $q = k$, i.e. substituting $q = k$ in the above equation, we obtained [21],

$$C = \frac{\int_0^\infty r^2 j_J(kr) \rho_{Jt_z}^{ms}(i,f,r) dr - Z F_J^L(k) \sqrt{\frac{2J_i+1}{4\pi}}}{\int_0^\infty r^{J+1} \rho_0(i,f,r) j_{J-1}(kr)\, dr}. \tag{11}$$

3. Results and Discussion

Calculations are presented 2^+ in ^{18}O and ^{22}Ne with excitation energies of 1.982 and 1.725 MeV, respectively, and 4^+ states in ^{20}Ne nuclei with excitation energies of 4.247 MeV. These calculations are performed using Wildenthal (W) and USDA effective interactions for the sd-shell model to generate the OBDM. These calculations are performed using the shell model Nushellx@MUS code [22]. The wave functions for single particles are those for the HO, WS, and SKX potentials. According to the sd-shell model concepts, it is described as an inert core of ^{16}O plus 2, 4,and 6 nucleons for ^{18}O, ^{20}Ne, and ^{22}Ne, respectively, which are distributed over the sd-shell. The comparison between the theoretical and experimental C2 and C4 form factors shows a goodagreement.

The longitudinal C2 form factors for 2^+ (1.982 MeV) state in ^{18}O nucleus calculated three potentials: HO, WS, and SKX on sd-shell model wave functions, which are shown in Figs. 1–5. The CP effects with the Tassie model and Bohr–Mottelson collective. The USDA interaction has been used to calculate the coulomb C2. Figures 1, 2, and 3 show a comparison between the calculated form factors with the inclusion of CP effects by the Tassie model

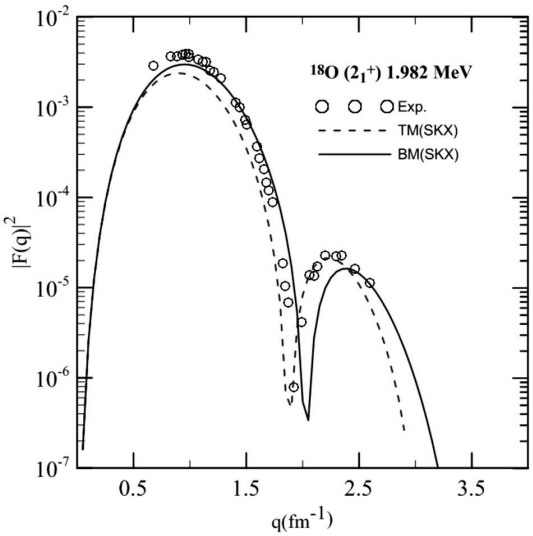

Fig. 3. The longitudinal C2 form factors for the transition of the 2_1^+ (1.982 MeV) state in ^{18}O, with the BM collective model and Tassie model (TM), with SKX potential

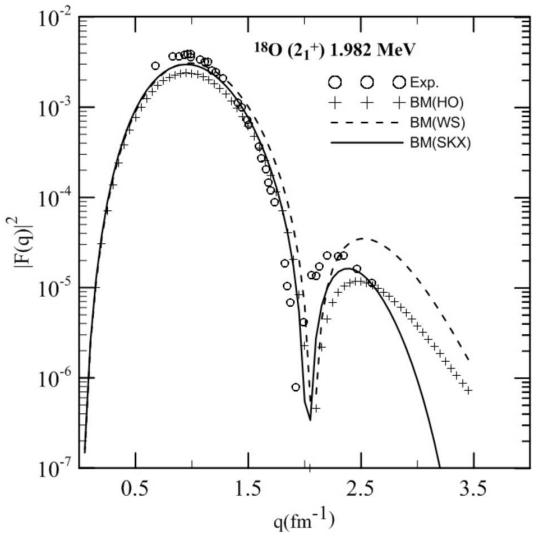

Fig. 5. The longitudinal C2 form factors for the transition of the 2_1^+ (1.982 MeV) state in ^{18}O, with the BM collective model, with HO, WS, and SKX potentials

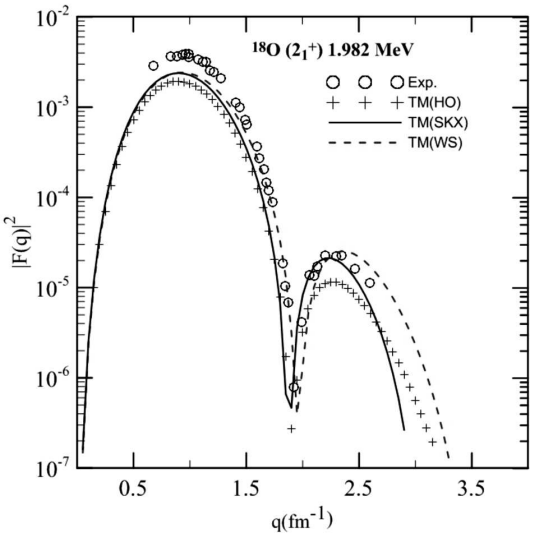

Fig. 4. The longitudinal C2 form factors for the transition of the 2_1^+ (1.982 MeV) state in ^{18}O, with the Tassie model, with HO, WS, and SKX potentials

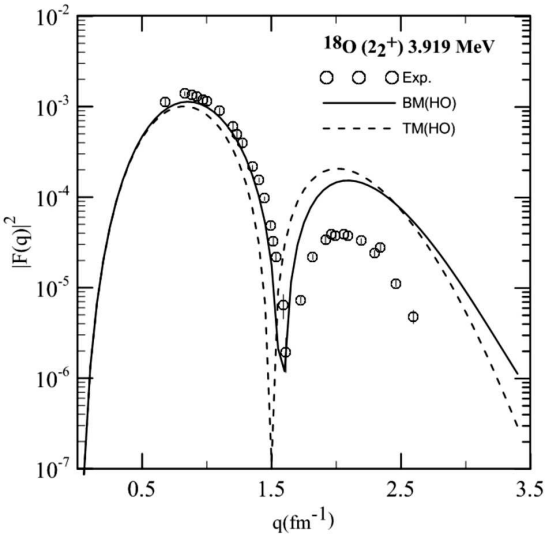

Fig. 6. The longitudinal C2 form factors for the transition of the 2_2^+ (3.919 MeV) state in ^{18}O, with the BM collective model and Tassie model (TM), with HO potential

(dashed curve) and BM model (solid curves) for three potentials. The C2 form factor with the BM model which is shown by the solid curve in Fig. 1, where the data are in a good agreement for the momentum transfer interval (1.5–2) fm^{-1} comparing with calculations with Tassie model. All calculations were performed using the HO wave function with size parameter $b = 1.80$ fm [23]. In Fig. 2, the calculations in the BM collective model with the WS potential give a good agreements for the momentum transfer interval between (0.5–1.6) fm^{-1} comparisons with the Tassie model, while TM enhances the form factor and reproduces the measured form factors in the region between $(1.6 < q < 2.5)$ fm^{-1}. Figure 3 shows that the inclusion of CP effects using the BM collective model with SKX potential give agreements

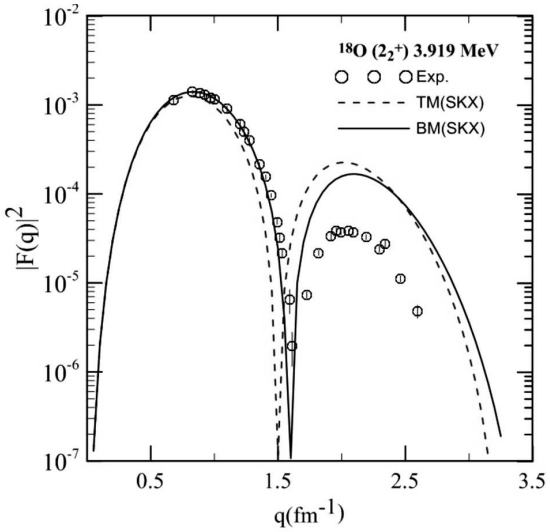

Fig. 7. The longitudinal C2 form factors for the transition of the 2_2^+ (3.919 MeV) state in ^{18}O, with the BM collective model and TM, with SKX potential

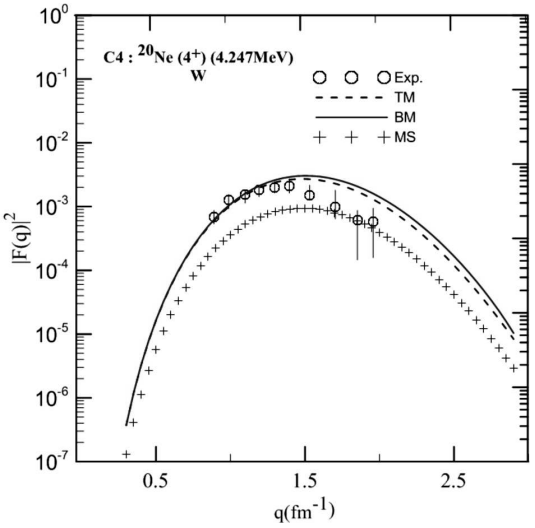

Fig. 8. The longitudinal C4 form factors for the transition of the 4_1^+ (4.247 MeV) state in ^{20}Ne, with the BM collective model and Tassie model (TM), with Wildenthal (W) effective interaction

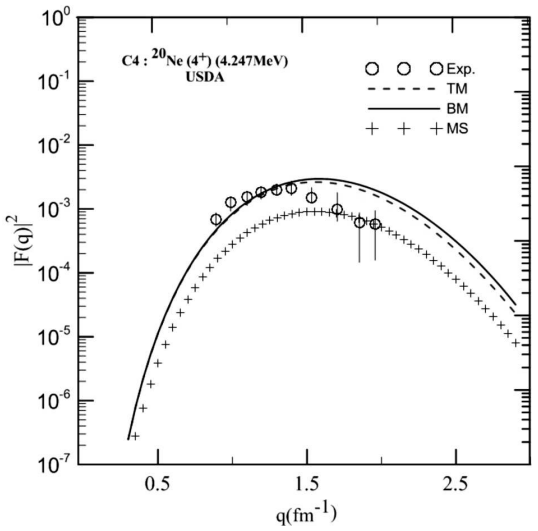

Fig. 9. The longitudinal C4 form factors for the transition of the 4_1^+ (4.247 MeV) state in ^{20}Ne, with the BM collective model and TM, with the USDA effective interaction

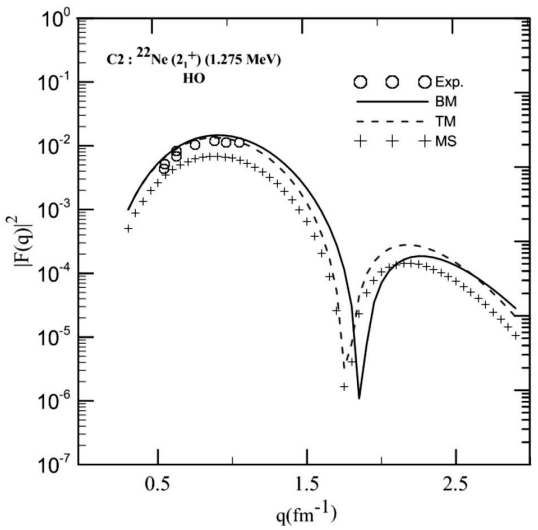

Fig. 10. The longitudinal C2 form factors for the transition of the 2_1^+ (1.275 MeV) state in ^{22}Ne, with the BM collective model and Tassie model, with the HO potential

with the experimental data for the first maximum region between (0.5–2) fm^{-1}, while, in the second maximum region (2–2.7) fm^{-1}, we observe that the TM gives a good agreement comparing with the BM collective model which fails to describe the experimental data [24].

The C2 form factors for 2_+^2 (3.919 MeV) state in ^{18}O nucleus are calculated with two potentials: WS and SKX in the sd-shell model wave function, which are shown in Figs. 4–7. In Fig. 4 and 5, which represented the relation between C2 form factor as a function of the momentum transfer, we notice that the calculations in the BM collective model with the HO and WS potentials give a good agreements in the first maximum momentum transfer region between (0.5–1.6) fm$^-$1, comparisons with the experimental data

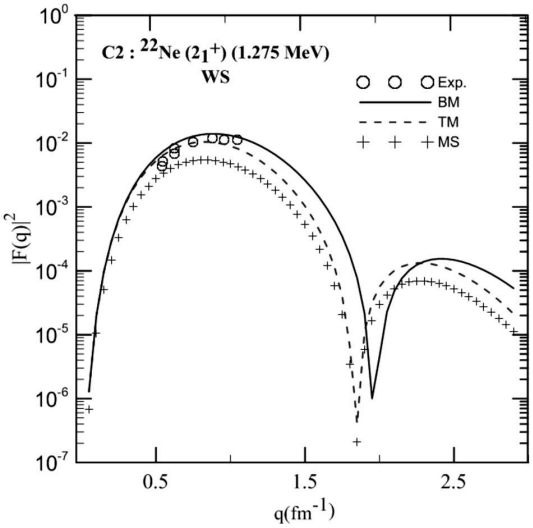

Fig. 11. The longitudinal C2 form factors for the transition of the 2_1^+ (1.275 MeV) state in ^{22}Ne, with the BM collective model and Tassie model, with the WS potential

interval between (0–2.5) fm$^-$1. The calculations with TM fails to describe the experimental data [24] in the whole momentum transfer region.

The longitudinal C4 form factors for 4_1^+ (4.247 MeV) state in ^{20}N nucleus with the HO potential. These calculations are performed using the Wildenthal (W) and USDA effective interactions for the sd-shell model to generate the OBDM. Figures 8, 9 show that the calculation with model space only fails to describe the experimental data up to a momentum transfer of 1.5 fm^{-1}, while the C4 form factors using the TM and BM collective models give agreements in the region of momentum transfer between (0.8–1.4) fm^{-1}. The model space after 1.5 fm^{-1} gives acceptable agreement with experimental data [25].

The Coulomb (C2) form factor as a function of the momentum transfer (q) for 2_+^1 (1.275 MeV) in ^{22}Ne is shown in Figs. 10 and 11, where the solid curve and dashed curve are represent calculations using the BM collective model and TM, respectively. These calculations are performed using the HO and WS potentials to calculate the wave functions of radial single-particle matrix elements. The theoretical results for the BM collective model and TM in first peak are successful to describe the experimental data [26] using the HO and WS potentials at the momentum transfer region between (0.5–1.3) fm^{-1}.

In general, the importance of the core polarization effects in some longitudinal components of form factors remains as an open question. The calculations with core polarization effects may be affected by some important parameters such as effective charges (protons and neutrons), the size parameters for the HO potential, the type of potentials and the type of effective charge which is used in calculations. However, our aim in this work is to study the BM collective model and TM contributions without adjusting any parameter.

4. Conclusions

Coulomb C2 form factors are calculate for 2^+ in ^{18}O and ^{22}Ne with excitation energies of 1.982 and 1.725 MeV, respectively, and C4 in ^{20}Ne nuclei with excitation energies 4.247 MeV. The Wildenthal (W) and USDB interactions for the sd-shell are used with the TM model and the BM collective one for the core polarization calculations. The core polarization effects on form factors with using the BM collective model and the TM one are found to be very needful in the calculations of the C2 and C4 form factors and gives good agreement over the sd-shell model calculations for the form factors. The results of C2 form factors for 2_1^+ (1.982 MeV) of ^{18}O fail to describe the experimental data in the second maximum region. The C4 results for 4_1^+ state for ^{20}Ne nucleus deviated from the experimental data at the momentum transfer region after 1.5 fm^{-1}. In this work, the calculations are performed without adjusting any parameter.

1. R.R. Roy, B.P. Nigam. *Nuclear Physics* (John Wiley and Sons, INC., 1967).
2. B.H. Wildenthal. Empirical strengths of spin operators in nuclei. *Progr. Part. Nucl. Phys.* **11**, 5 (1984).
3. E.K. Warburton, B.A. Brown. Effective interactions for the $0p1s0d$ nuclear shell-model space. *Phys. Rev. C* **46**, 923 (1992).
4. E.K. Warburton, J.A. Becker, B.A. Brown. Mass systematics for $A = 29$–44 nuclei: The deformed $A \sim 32$ region. *Phys. Rev. C* **41**, 1147 (1990).
5. Yu. Utsuno, T. Otsuka, T. Mizusaki, M. Honma. Varying shell gap and deformation in $N \sim 20$ unstable nuclei studied by the Monte Carlo shell model.*Phys. Rev. C* **60**, 054315 (1999).
6. S. Nummela, P. Baumann, E. Caurier *et al.* Spectroscopy of ^{34,35}Si by β decay: *sd-fp* shell gap and single-particle states. *Phys. Rev. C* **63**, 044316 (2001).
7. B.A. Brown, W.A. Richter. New "USD" Hamiltonians for the *sd* shell. *Phys. Rev. C* **74**, 034315 (2006).

8. G. Bertsch, J. Borysowicz, H. McManus, W.G. Love. Interactions for inelastic scattering derived from realistic potentials. *Nucl. Phys. Section A* **284**, 399 (1977).
9. W.A. Richter, B.A. Brown. ^{26}Mg observables for the USDA and USDB Hamiltonians. *Phys. Rev. C* **80**, 034301 (1992).
10. A.R. Ridha, M.K. Suhayeb. Theoretical study of nuclear density distributions and elastic electron scattering form factors for some halo nuclei. *Iraqi J. Phys.* **58**, 2098 (2107).
11. J. Liu, Ch. Xu, Sh. Wang, Zh. Ren. Coulomb form factors of odd-A nuclei within an axially deformed relativistic mean-field model. *Phys. Rev. C* **96**, 034314 (2017).
12. R.A. Radhi, A.K. Hamoudi, S.K. Jassim. Calculations of longitudinal form factors ofp-shell nuclei, using enlarged model space including core-polarization effects with realistic two-body effective interaction. *Indian J. Phys.* **81**, 683 (2007).
13. K.S. Jassim, A.A. Al-Sammarrae, F.I. Sharrad, H. Abu Kassim. Elastic and inelastic electron-nucleus scattering form factors of some light nuclei: ^{23}Na, ^{25}Mg, ^{27}Al, and ^{41}Ca. *Phys. Rev. C* **89**, 014304 (2014).
14. K.S. Jassim, R.A. Radhi, N.M. Hussain. Inelastic magnetic electron scattering form factors of the ^{26}Mg nucleus. *Pramana J. Phys.* **86**, 87 (2016).
15. K.S. Jassim. The electron scattering form factor of ^{10}B, ^{32}S and ^{48}Ca nucle. *Physica Scripta* **86**, 035202 (2012).
16. K.S. Jassim, A.I. Faris. Study of nuclear structure of ^{58,62}Ni isotopes using the F5PVH effective interaction. *Int. J. Nucl. Energy Sci. Techn.* **13**, 261 (2019).
17. K.S. Jassim, S.R. Sahib. Large-scale shell model calculations of the ^{25,26}Mg, ^{27}Al and ^{19}F nucleus. *Int. J. Nucl. Energy Sci. Techn.* **12**, 81 (2018).
18. K.S. Jassim. Nuclear structure of ^{104,106,108}Sn isotopes using the NuShell computer code. *Chinese J. Phys.* **51**, 441 (2013).
19. L. Tassie. A model of nuclear shape oscillations for g? Transitions and electron excitation. *Australian J. Phys.* **9** (4), 407 (1956).
20. T. de Forest, Jr., J.D. Walecka. Electron scattering and nuclear structure. *Advan. Phys.* **15**, 1 (1966).
21. J. Heisenberg, J.Mc. Carthy, I. Sick. Inelastic electron scattering from several Ca, Ti and Fe isotopes. *Nucl. Phys. A* **164**, 353 (1971).
22. B.A. Brown, M. Rae. NuShellMSU. *MSU-NSCL report* **524**, 1 (2007).
23. B.A. Brown, W. Chung, B.H. Wildenthal. Electromagnetic multipole moments of ground states of stable odd-mass nuclei in the *sd* shell. *Phys. Rev. C* **22** (2), 774 (1980).
24. B.E. Norum, M.V. Hynes, H. Miska, W. Bertozzi, J. Kelly, S. Kowalski, F.N. Rad, C.P. Sargent, T. Sasanuma, W. Turchinetz. Inelastic electron scattering from ^{18}O. *Phys. Rev. C* **25**, 1778 (1982).
25. Y. Horikawa, Y. Torizuka, A. Nakada, S. Mitsunobu *et al.* The deformations in ^{20}Ne, ^{24}Mg and ^{28}Si from electron scattering. *Phys. Lett. B* **36**, 9 (1971).
26. X.K. Maruyama, F.J. Kline, J.W. Lightbody *et al.* Electroexcitation of ^{22}Ne below $E_x = 8.6$ MeV. *Phys. Rev. C* **19**, 1624 (1979).

Received 12.03.20

І.А.Х. Аджіл, М.Дж.Р. Адухайбат, К.С. Джассім

КУЛОНІВСЬКІ C2 ТА C4
ФОРМФАКТОРИ ЯДЕР ^{18}O, ^{20,22}Ne
У КОЛЕКТИВНІЙ МОДЕЛІ БОРА–МОТТЕЛЬСОНА

В рамках оболонкової моделі розраховано кулонівські C2 та C4 формфактори ядер ^{18}O і ^{20,22}Ne з урахуванням ефектів від поляризації кора в 2^+ та 4^+ станах ^{18}O і ^{20,22}Ne ядер розраховані в рамках оболонкової моделі. Використано двочастинкову ефективну взаємодію Вілденталя і універсальну взаємодію A в *sd*-оболонці (USDA). Для розрахунку ефектів від поляризації кора використано модель Тассі з кулонівською взаємодією та колективну модель Бора–Моттельсона. Для потенціалів гармонічного осцилятора, Вуда–Саксона та SKX знайдено хвильові функції, які входять до радіальних одночастинкових матричних елементів. Врахування ефектів від поляризації кора дає краще узгодження з експериментальними даними в порівнянні з іншими просторовими моделями. Співставлено результати для різних потенціалів.

Ключові слова: ядра з *sd*-оболонкою, поздовжні формфактори, кулонівські формфактори, програмний код Nushellx@MUS.